https://doi.org/10.5194/amt-2023-175
Preprint. Discussion started: 4 October 2023

Atmospheric Measurement Techniques Discussions

Improved rain event detection in Commercial Microwave Link time series via combination with MSG SEVIRI data

Andreas Wagner[1], Christian Chwala[2], Maximilian Graf[1], Julius Polz[2], Llorenç Lliso[3], José Alberto Lahuerta[3], and Harald Kunstmann[1,2]

[1]University of Augsburg, Institute of Geography (IGUA), Alter Postweg 118, 86159 Augsburg, Germany
[2]Karlsruhe Institute of Technology, Campus Alpin (IMK-IFU), Kreuzeckbahnstraße 19, 82467 Garmisch-Partenkirchen, Germany
[3]Agencia Estatal De Meteorología (AEMET Spain)

Correspondence: Christian Chwala (christian.chwala@kit.edu)

Abstract. The most reliable areal precipitation estimation is usually generated via combinations of different measurements and devices by merging their individual advantages. Path-averaged rain rate can be derived from Commercial Microwave Links (CML), where attenuation of the emitted radiation is strongly related with rainfall rate. CMLs can be combined with data from other rainfall measurements or used individually. They are available almost worldwide and often represent the only opportunity of ground-based measurement in data scarce regions. Deriving rainfall estimates from CML data requires extensive data processing, though. The separation of the attenuation time series in rainy and dry periods (rain event detection) is the most important step in this processing and largely determines the quality of the resulting rainfall estimates. In this study, we investigate the suitability of Meteosat Second Generation Spinning Enhanced Visible and InfraRed Imager (MSG SEVIRI) satellite data as an auxiliary-data-based (ADB) rain event detection method. We compare this method with two time-series-based (TSB) rain event detection methods. The investigation uses data from 3901 CMLs in Germany for four months in summer 2021 and is carried out for the two SEVIRI-derived products PC and PC-Ph. We analyse all rain event detection methods for different precipitation intensity, differences between day and night, as well as their influence on the performance of rainfall estimates from individual CMLs. The radar product RADKLIM-YW is used for validation. The results show that both SEVIRI products are promising candidates for ADB rainfall detection methods and led to at least equivalent results as the TSB methods. The main uncertainty of all methods was found for light rain. Slightly better results were obtained during the day than at night, which is caused by dew formation on CML antennas and the reduced availability of SEVIRI channels at night. In general, the ADB methods lead to improvements for CMLs performing comparatively weakly using TSB methods. Based on these results, combinations of ADB and TSB methods were developed by emphasizing their specific advantages. Compared to basic and advanced TSB methods, these combinations were able to improve the Matthews Correlation Coefficient of the rain event detection from 0.53 (0.57 resp.) to 0.62 during the day and from 0.47 (0.55 resp.) to 0.6 during the night. Our results show that utilising MSG SEVIRI data in CML data processing significantly increases the quality of the rain event detection step, in particular for CMLs which are challenging to process with TSB methods.

https://doi.org/10.5194/amt-2023-175
Preprint. Discussion started: 4 October 2023

Atmospheric Measurement Techniques Discussions

1 Introduction

Precipitation is the most important variable for hydrology and water management. It is characterized by a high variability in space and time, especially in the case of convective rain events. The quality of hydrological modeling results depends heavily on high-resolution and reliable areal precipitation (Fu et al., 2011; Bruni et al., 2015; Rafieeinasab et al., 2015; Cristiano et al., 2017). There are a variety of rainfall measurement methods which serve as a basis for the derivation of rainfall fields, each with specific advantages but also drawbacks. Tipping buckets for instance usually provide the best point measurements of precipitation, but they are prone to errors due to wind and evaporation (Sevruk, 2006) and primarily lack spatial representativeness (Pollock et al., 2018). Satellite data provide areal precipitation patterns almost worldwide with a spatial resolution in the order of several kilometers. But they either suffer from poor temporal resolution (the GPM core satellite has a revisit time of approximately 1 day in the tropics) or from heterogeneous data quality and delayed availability (merged satellite products like IMERG) (Hou et al., 2014). Additionally, complex retrieval and calibration algorithms have to be applied which cause additional uncertainties (Maggioni et al., 2016). Weather radars derive areal precipitation patterns with a high resolution of 5 minutes and 1 km (Atlas, 1990; Bartels et al., 2004; Winterrath et al., 2012). However, the calculation of rain rate from radar reflectivity is non-trivial (Uijlenhoet et al., 2003; Steiner et al., 2004) and false echoes, clutter and other measurement effects cause further problems (Villarini and Krajewski, 2010; Wagner et al., 2012; Wagner, 2018). Schleiss et al. (2020) showed that radar data tends to underestimate particularly heavy rainfall. Nevertheless, gauge-adjusted radar data is considered to be the best possible data basis (Bartels et al., 2004; Winterrath et al., 2012). It is precisely the combination of different measurements that makes it possible to leverage the advantages and neglect disadvantages of individual systems.

The opportunistic sensing of precipitation is becoming available on country-wide scales (Overeem et al., 2016; Graf et al., 2021). One example is the use of attenuation data from Commercial Microwave Links (CML) measurements to determine precipitation. It was first initiated in Israel (Messer et al., 2006) and the Netherlands (Leijnse et al., 2007). Attenuation of CML data is a disturbing effect for the operating telecommunication providers but can be used to calculate precipitation intensity. The relationship between attenuation and precipitation is significantly more linear for signals between 10 and 40 GHz than between radar reflectivity and precipitation (Atlas and Ulbrich, 1977). Correspondingly, the line integrals of precipitation can complement conventional measurement methods (Liberman et al., 2014; Haese et al., 2017; Graf et al., 2021). Kumah et al. (2022) for instance derived rain intensities from MSG satellite data by a random forest algorithm trained with CML rainfall estimates. However, a number of publications confirm that CML data is also applicable as the only source for areal precipitation (Overeem et al., 2013; Rios Gaona et al., 2015; Overeem et al., 2016; D'Amico et al., 2016; Graf et al., 2020; Roversi et al., 2020; van de Beek et al., 2020). In large areas of Africa, for instance, radar data and even station data is missing or only sparsely available, so a mobile phone network might be the only addition to satellite data. The importance of CML can therefore be rated much higher there. Chwala and Kunstmann (2019) and Uijlenhoet et al. (2018) give an overview of challenges and background information on the usage of CML data as a source of precipitation measurements. CML data is affected by reflection of the beam, dew formation on the antenna or fog which can be wrongly interpreted as precipitation echoes. Changes in propagation characteristics due to the influence of water vapour or temperature and drifts in signal characteristics due to

https://doi.org/10.5194/amt-2023-175
Preprint. Discussion started: 4 October 2023


Atmospheric Measurement Techniques Discussions

strong solar radiation or air temperature cause further non-precipitation variations of the signals (Chwala and Kunstmann, 2019). Therefore, the rain event detection is a major step in estimating rainfall rates from CML signals. The different available approaches are "individual methods" for rain event detection, since they are based only on one method or data set. They can roughly be divided into time series-based (TSB) methods and methods based on auxiliary data of precipitation patterns (ADB).

The TSB methods include the simple threshold models (Leijnse et al., 2008), the rolling standard approach (RS) (Schleiss and Berne, 2010) and more complex ones such as Markov switching models (Wang et al., 2012) and short-term Fourier Transform approaches (Chwala et al., 2012). Messer and Sendik (2015) provide a detailed description of these approaches. Machine Learning approaches to distinguish between wet and dry time steps emerged in recent years, usually outperforming the previous methods (Habi and Messer, 2018; Polz et al., 2020; Song et al., 2020) The "nearby-link" approach (Overeem et al., 2016) is usually not viewed as a TSB, but nevertheless uses CML attenuation time series by comparing neighboring CMLs regarding attenuation effects within a radius of 15 km.

Regarding ADB approaches, best results are usually achieved with radar data (Overeem et al., 2011), but satellite data is also used (van het Schip et al., 2017; Kumah et al., 2021). Geostationary satellites such as MSG SEVIRI offer a temporal resolution of 15 minutes at 4x6 km spatial resolution in mid-latitudes. This data is also used as areal precipitation (Roebeling et al., 2008; Roebeling and Holleman, 2009), although the derivation of precipitation from VIS and IR channels is often uncertain. According to NWC SAF (Lahuerta García, 2021) even a distinction between light, moderate and heavy precipitation is difficult. That is the reason why they determine the probability of precipitation in their post-processed SEVIRI products. However, such a product can be very useful as an indicator whether it is raining or not. van het Schip et al. (2017) has carried out analyzes applying post-processed SEVIRI products as a wet-dry indicator in the Netherlands. A short period of 12 days is analyzed with focus only on rainfall maps not allowing any conclusion on individual CMLs and their specific rain event detection performance. Their satellite approach performs better than doing the CML processing without a rain event detection, but worse than the radar-based rain event detection approach. So, it is not straightforward to evaluate the quality of their approach compared to standard rain event detection approaches. In addition, there is no differentiation according to precipitation intensity or between day and night, although there are no visual channels at night and the satellite product methodologically varies greatly. Kumah et al. (2021) obtained improved rain intensities for convective rain events when applying MSG SEVIRI data for rain event detection of CML data. However, their results are based only on one CML in Kenya for daytime and rain intensities above 0.5 mm/h.

In this study, two precipitation products (PC and PC-Ph) from NWCSAF derived from the SEVIRI radiometer on-board the geostationary satellite METEOSAT are applied for rain event detection. In addition to comparing ADB (based on the PC and PC-Ph products) and TSB (CML time series processing) methods, this study presents a novel way of combining TSB and ADB rain event detection approaches to improve rain event detection. In order to analyze the applicability of such new rain event detection methods, data sets of high data quality are necessary. The present analysis is based on country-wide CML data from 4 months in summer 2021 in Germany and a high-resolution gauge-adjusted radar product is used as reference.

https://doi.org/10.5194/amt-2023-175
Preprint. Discussion started: 4 October 2023

Atmospheric Measurement Techniques Discussions

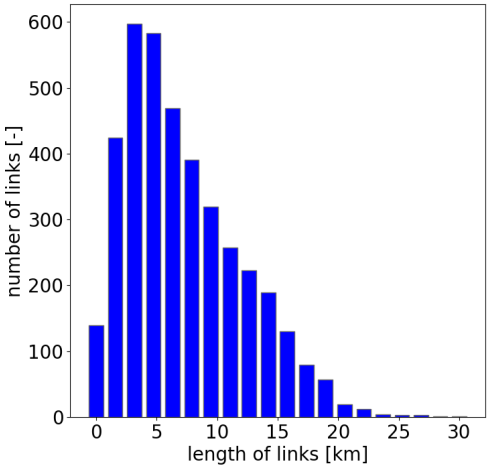

Figure 1. Histogram revealing the distribution of length of the 3901 CMLs in Germany.

The research questions of this investigation are: (1) are PC and PC-Ph products suitable as a wet-dry indicator for CML data? (2) Do the results vary with rain intensity? (3) Are there noticeable differences between day and night? (4) Can a combination of TSB and ADB rain event detection methods outperform TSB-only and ADB-only methods?

2 Data

The evaluations in this study are based on CML data, radar data and SEVIRI data in Germany for a period of 19 weeks between 31st of May 2021 and 10th of October 2021.

2.1 CML data

3901 CMLs in Germany are used, which are operated by Ericsson. This is only a subset of all CMLs operated in Germany. The path lengths of the CMLs vary between 0.2 km and about 30 km (see Fig. 1). 72 % are shorter than 10 km and over 99 % are shorter than 20 km. The frequencies typically range between 10 and 40 GHz with shorter CMLs using higher frequencies. The transmitted signal level (TSL) with a power resolution of 1 dB and the received signal level (RSL) with a power resolution of 0.3 dB are saved every minute using a custom real-time CML data acquisition system (Chwala et al., 2016). The processing of the data is described in more detail in chapter 3.1.

2.2 Radar data

RADKLIM-YW is a gauge-adjusted, climatologically-corrected radar product of the German Meteorological Service (DWD) and it is used to validate SEVIRI and CML data. An adjustment to hourly data from precipitation stations similar to that of

https://doi.org/10.5194/amt-2023-175
Preprint. Discussion started: 4 October 2023


Atmospheric Measurement Techniques Discussions

the more well-known *RADOLAN-RW* product is used (Bartels et al., 2004; Winterrath et al., 2012), but the *RADKLIM-YW* data is available every 5 minutes. In addition, climatologically-based corrections of spokes and range-dependencies are carried out (Winterrath et al., 2018). According to Kreklow et al. (2020), the range-dependent effects, which are particularly strong in winter, are reduced. This improves precipitation patterns and better represents orography compared to *RADOLAN-RW*. At the same time, however, a slight underestimation of the total precipitation was determined.

2.3 SEVIRI data

The Spinning Enhanced Visible and Infrared Imager (SEVIRI) radiometer from the geostationary satellite METEOSAT provides image data in two Visible (VIS), one high resolution channel (HRVIS) and nine Infrared (IR) channels including also one Near Infrared channel (NIR). The channels range from 0.5 to 14.4 micrometres with a resolution of 3 km at the sub-satellite point. The high-resolution channel is not used for our purposes. Every 15 minutes the image of the full earth disc (lon: -79°-79°, lat: -81° - 81°) is available including calibration (Schmid, 2000). No specific device for precipitation measurement is on-board, such as for GPM (Hou et al., 2014). The derivation of precipitation products is based on two approaches: either by regression of different channels and adjustment to precipitation measurements or, more sophisticated, through the derivation of microphysical parameters (Roebeling et al., 2008; Hernanz et al., 2019). For the calculation of microphysical parameters, the 0.6 um channel (VIS) and the 1.6 um channel (NIR) is mandatory (Roebeling et al., 2008). The first product PC-Ph is derived from the microphysical parameters Effective Radius (Reff) and Cloud Optical Thickness (COT) at daytime. At night, when visible channels are missing, it is calculated by a regression of IR and Water Vapour channels (WV). The second product PC relies on different regression functions of available SEVIRI channels, also including VIS, IR and WV channels at daytime and only IR and WV channels at night. Both products provide the probability of precipitation in percent: PC in increments of 10 and PC-Ph in increments of 1. A detailed description of the respective products and their validation can be found at Thoss (2014); Hernanz et al. (2019); Lahuerta García (2019)

3 Methods

3.1 CML data processing

The processing of CML data must be handled with care. Various groups developed CML processing methods that depend on e.g. the sampling strategy. In Germany, TSL and RSL of about 4000 CMLs are sampled instantaneously with a temporal resolution of 1 minute. Missing or corrupted data reduces the amount to 3901 CMLs used in this evaluation. Each CML has two sublinks which each have one TSL and RSL time series. From a purely practical point of view, we only processed data from the first sublink. A more detailed description of the processing of the data can be found in Graf et al. (2020). The most important aspects of data processing are briefly outlined in the following.

https://doi.org/10.5194/amt-2023-175
Preprint. Discussion started: 4 October 2023


Atmospheric Measurement Techniques Discussions

The high temporal resolution of the raw data is preserved for the processing of the data. Gaps of up to 5 minutes due to missing time steps or measurements are interpolated to obtain continuous time series. The total path loss along the CML (TRSL) is then calculated as TSL minus RSL.

As a next step, wet and dry time steps have to be detected (rain event detection). This might be difficult, if attenuation signals from noise and precipitation are very similar. High similarities occur for very low rain intensities or noisy CML data. Overestimation of total precipitation and of the number of wet time steps result if noise is classified as precipitation. Underestimation occurs if time steps with precipitation are missed. Consequently, the reliable separation of precipitation-induced attenuation and noise from fluctuations in TRSL largely determines the quality of CML data. Being the central element of this manuscript, it will be discussed individually in Chapter 3.2.

Then, the baseline attenuation is dynamically identified for the preceding dry period of each rain event in order to derive the rainfall induced attenuation along the path. This baseline is the last dry time-step of the TRSL time-series and is set to be constant during the rain event.

The resulting attenuation may be overestimated due to wetting effects on the radome. To overcome this problem, a correction of this wet antenna attenuation (WAA) according to Leijnse et al. (2008) is used. In this physical approach, the dependence of WAA on antenna cover properties (refractive index and thickness), microwave frequency and rain intensity is defined. The original parameters from Leijnse et al. (2008) are adopted.

The corrected attenuation from CML was used to derive the precipitation rate using a k-R relationship in the form of a power-law fit to drop-size-distribution simulations. The parameter settings were based on ITU recommendations (ITU-R, 2005) with a close-to-linear relationship between attenuation and rain rate. According to Chwala and Kunstmann (2019); Graf et al. (2020) they show good agreements for Germany.

3.2 Rain event detection

3.2.1 Individual methods for rain event detection

Two time series based (TSB) methods for rain event detection are applied for comparison. The first one is the Rolling Standard Deviation method (*RS*) according to Schleiss and Berne (2010), modified by Graf et al. (2020). Based on this approach, the threshold is determined based on the 80th percentile of a 60 min rolling standard deviation multiplied by a scaling factor. The constant scaling factor of 1.12 is adopted from Graf et al. (2020) and was also used by Polz et al. (2020). The second one is a machine learning approach based on Convolutional Neural Networks from Polz et al. (2020) which is called *CNN* in the following. The classification threshold of 0.82 was adopted. Both approaches were compared in Polz et al. (2020) with significantly better performance of *CNN* compared to *RS*.

The use of SEVIRI data as a wet/dry indicator can be applied based on different precipitation probabilities. We use the thresholds 40 %, 30 %, 20 %, 10 % and 0.1 %. The last threshold represents probabilities greater than 0 %. The abbreviations for the thresholds are e.g., *P40* or *P01* and the abbreviations for the specific data sets of PC and PC-Ph are e.g., *PC10* or *PC-Ph20*. Before SEVIRI data can be used as a wet/dry indicator, the SEVIRI pixels must be remapped to the CML paths.

https://doi.org/10.5194/amt-2023-175
Preprint. Discussion started: 4 October 2023


Atmospheric Measurement Techniques Discussions

This is done by a weighted-averaging, where the weights are determined from the proportion of the CML length covered by the respective SEVIRI pixels. If several pixels are involved, the probability of precipitation often deviates from the original binning into 1 % and 10 % steps. Because of the 15-minute resolution of SEVIRI data, the probability is kept constant for 15 1-minute time steps of CML data.

3.2.2 Combinations of rain event detection methods

According to Polz et al. (2020) it is hardly possible to detect light rain events and accurately define dry periods in CML data at the same time. All existing rain event detection methods use a threshold that allows to choose between a more liberal detection (with better detection of small events but at the expense of more false positives) or a more conservative one (with better detection of dry periods, but at the expense of more false negatives). In the end, a compromise is unavoidable. This is not necessarily the case when combinations of different methods are applied. In order to exploit the advantages of different methods, a combination seems to be particularly promising if auxiliary-data-based (ADB) methods are used in addition to TSB methods. For the implementation, those time steps which can be classified dry or wet with a high degree of reliability have to be identified in both approaches. The challenge is defining the specific threshold and deciding when and where one method is more reliable than the other one.

In this study we apply a combination of different rain event detection variants, using different thresholds, for the TSB method *CNN* and the ADB method based on PC-Ph SEVIRI data. Each rain event detection variant is first calculated independently on raw CML data. The reasoning of our approach is that dry time steps in a very wet (liberal) variant of a rain event detection are most likely also dry in reality, and vice versa for wet predicted time steps in a very dry (conservative) variant. The rain event detection of these highly reliable time steps is adopted and used to overrule the classification as wet or dry generated from a previously calculated default rain event detection, which has only a lower confidence.

Our procedure of combining the rain event detection variants consists of 5 individual steps shown in Fig. 2. In step 1, we choose a method (either CML-TSB or SEVIRI-ADB) that shows a good average performance as a first guess. Step 2 and 5 use wet variants of both data sets and provide additional high-confidence dry time steps. Step 3 and 4 derive additional high-confidence wet time steps from dry variants of both data sets. Since later steps can modify earlier classifications of wet and dry time steps, the priority of the individual steps increases. The order of steps 2-5 might be changed but it is recommended that two conservative and two liberal variants are applied. The chosen individual combinations are mentioned in Chapter 4.3.

3.3 Statistical measures

The Pearson correlation PCC is used to evaluate the shape and temporal agreement of different precipitation time series. Focusing only on whether wet and dry time steps match between different data sets leads to categorical scores based on a confusion matrix (see equation 1):

https://doi.org/10.5194/amt-2023-175
Preprint. Discussion started: 4 October 2023

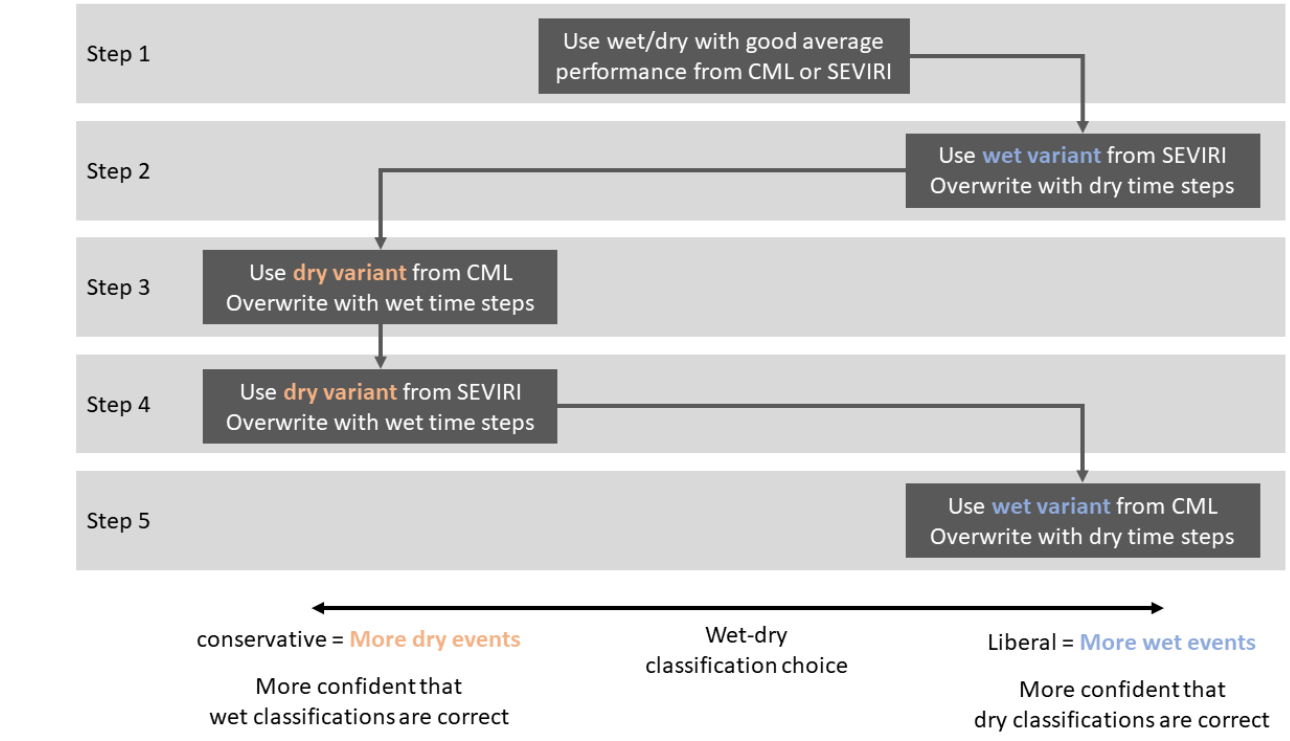

Figure 2. Flow chart for building a combination based on two different rain event detection methods. In this step-wise approach, which starts from a mean variant, only reliable wet (resp. dry) time steps derived from both methods are used to modify the mean variant based on a dry (resp. wet) variant.

$$\begin{pmatrix} TP & FP \\ FN & TN \end{pmatrix} = \begin{pmatrix} WET/wet & DRY/wet \\ WET/dry & DRY/dry \end{pmatrix} \tag{1}$$

with uppercase and lowercase denoting observed event and prediction, respectively. The number of correctly assigned wet time steps are called True Positives (TP) and the correctly assigned dry ones True Negatives (TN). False Positives (FP) represent the number of time steps where rain event detections are incorrectly assigned wet time steps and False Negatives (FN) represent the number of incorrect dry time steps. The True Positive Rate (TPR), the Positive Predictive Value (PPV), the Accuracy Correlation Coefficient (ACC) and the Matthews Correlation Coefficient (MCC) were selected from a large number of possible categorical statistical measures.

$$TPR = \frac{TP}{(TP + FN)} \tag{2}$$

https://doi.org/10.5194/amt-2023-175
Preprint. Discussion started: 4 October 2023


Atmospheric Measurement Techniques Discussions

$$PPV = \frac{TP}{(TP+FP)} \tag{3}$$

$$ACC = \frac{(TP+TN)}{(TP+FP+FN+TN)} \tag{4}$$

$$MCC = \frac{(TP \cdot TN - FP \cdot FN)}{\sqrt{(TP+FP)(TP+FN)(TN+FP)(TN+FN)}} \tag{5}$$

The TPR is the probability that an actual positive (wet time step) will also test positive. For the PPV only the positive values (TP and FP) are used. It is applied to show how "wet" a certain data set is. ACC compares the true values to the total population. According to Polz et al. (2020) it depends on the class balance. With a precipitation probability of 5-10 % in Germany, the majority of time steps are dry. Due to this skewed distribution the main focus of the analysis is based on the MCC which is affected much less by unbalanced distributions. The MCC is high, if both wet and dry classes are well represented.

3.4 Intensity classes

Despite the methodologically different rain event detections, the separation of dry and wet time steps is usually easier in the case of heavy precipitation since either the precipitation signal differs more clearly from the baseline CML signal or auxiliary precipitation data can more easily detect heavy precipitation. In order to confirm the assumption that heavy precipitation is easier to detect than light precipitation and to be able to evaluate the performance for different intensities, four additional intensity classes are applied in addition to the total precipitation. The classes for light, moderate and heavy precipitation are based on the (DWD, 2023) classification. "Light" precipitation is subdivided into two classes. This results in the five classes for "light1", "light2", "moderate", "heavy" and "total" precipitation shown in Tab. 2. Accordingly, the lower threshold for precipitation in this analysis is 0.1 mm/h and values below are considered dry.

Table 1. Overview of rain intensity classes for evaluations

Title	**light1**	**light2**	**moderate**	**heavy**	**total**
intensity [mm/h]	0.1 – 1.0	1.0 – 2.5	2.5 – 10.0	> 10.0	>= 0.1

4 Results and Discussion

We compared raw SEVIRI products with RADKLIM-YW to assess its suitability as a ADB wet/dry indicator for CML data. Then, we analyzed the performance of CML rainfall derived with a total of eight TSB and ADB rain event detection methods.

https://doi.org/10.5194/amt-2023-175
Preprint. Discussion started: 4 October 2023


Atmospheric Measurement Techniques Discussions

Based on these results, we created six TSB and ADB combinations and evaluated their performance compared to individual TSB and ADB methods. Finally, we investigated the influence of different rain event detection methods on the performance of individual CMLs.

4.1 Performance of raw SEVIRI products

To assess the quality of SEVIRI data it was directly compared to radar data. At this first step, no CML data was involved, but both data sets have been path-averaged along the CML paths.

In Fig. 3a, TPR shows the percentage of wet *RADKLIM-YW* time steps per intensity class and precipitation amount, represented by SEVIRI data for different thresholds. The largest differences were obtained for small intensities. While for *P01* around 80 % of the wet *RADKLIM-YW* time steps were correctly assigned wet, this proportion decreased to around 20 % for *P30*. For higher intensities, the proportion was over 90 % for *P01* and roughly 60 % for *P30*. In this way, 90 % of *RADKLIM-YW*'s precipitation amount was covered by *P01* and only 50 % by *P30*. Differences between day and night existed, but the general behavior over different rain intensity was similar.

According to TPR (blue column) in Fig. 3b, a maximum of 80 % of the wet time steps (according to radar data) are also classified wet by SEVIRI (*P01*). However, this corresponds to only 25 % (nighttime) and 40 % (daytime) of the total SEVIRI wet time steps (*P01*, PPV). Consequently, *P01* showed more wet time steps than the radar data. *P30* showed the opposite. This was also reflected in the performance metrics ACC and MCC. The best performance based on MCC was achieved by *P10* as a compromise between coverage of wet radar time steps and a meaningful number of wet and dry time steps. MCC was 0.53 during the day and 0.42 at night. This difference can probably be attributed to the missing SEVIRI channels at night. Although the results between PC and PC-Ph were similar, there were slight tendencies: PCC revealed a significantly better performance for PC-Ph than for PC. ACC showed similar tendencies, while the results for MCC were inconclusive.

According to these analyses, *P01* and *P10* are promising candidates representing *RADKLIM-YW* precipitation. The direct comparison of SEVIRI data and radar data was only of limited significance since the combination of CML raw data signals and satellite information is important when using SEVIRI as a wet/dry indicator. So, the next step was to analyze CML data based on SEVIRI and the TSB rain event detection methods *RS* and *CNN*.

4.2 Evaluation of individual methods for rain event detection

Eight different rain event detection methods were used within one CML processing routine described in Chapter 3.1 and the resulting data sets were compared to the reference *RADKLIM-YW*. First, they were evaluated based on the frequency of rainfall occurrence and total precipitation amount. This described the average behaviour, but did not allow to draw any conclusions on the temporal correspondence of CML data sets and radar data. For this purpose, statistical measures based on the confusion matrix were compared in the second part of this subsection.

https://doi.org/10.5194/amt-2023-175
Preprint. Discussion started: 4 October 2023

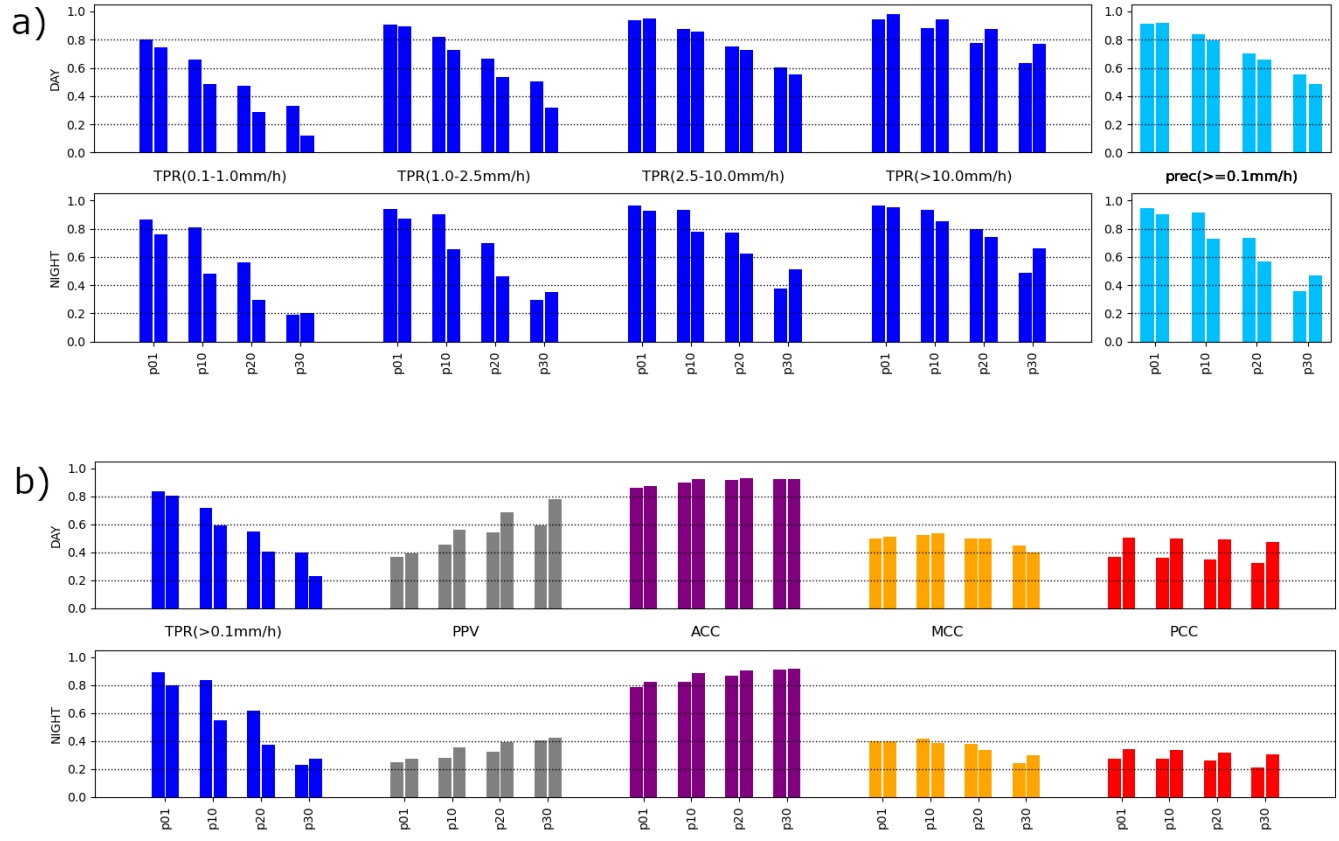

Figure 3. a) TPR of SEVIRI data and *RADKLIM-YW* per intensity class and the resulting *RADKLIM-YW* precipitation amount represented by PC (left column) and PC-Ph (right column) for SEVIRI rain probabilities from *P01* to *P30* for day (top) and night (bottom). b) respective TPR without subdivision into intensity classes and the statistical performance measures PPV, ACC, MCC and PCC.

4.2.1 Effect of rain event detection on total counts of wet time steps and precipitation

The distribution of rain intensities and total precipitation amount of eight rain event detection methods is shown in Fig.4. Overall, all rain event detection methods underestimated the occurrence of light precipitation and overestimated the occurrence of heavy precipitation, albeit with a general lower frequency of occurrence for the latter. Since all data sets showed this tendency, this can be attributed more to the general performance of CML data than to the rain event detection method. This behaviour probably resulted from both the WAA correction tending to correct too many small intensities (Graf et al., 2020), and a tendency of radar data to underestimate heavy rain intensities (Schleiss et al., 2020). The SEVIRI-based ADB data sets behaved very similarly to the two TSB data sets *RS* and *CNN*. The chosen probability level of SEVIRI data dominated the behaviour with a clear decrease of rainfall occurrences with higher precipitation probabilities. For ADB methods the night is slightly wetter than the day and a similar tendency occurred in the TSB data sets. Regarding precipitation amounts, the TSB

https://doi.org/10.5194/amt-2023-175
Preprint. Discussion started: 4 October 2023

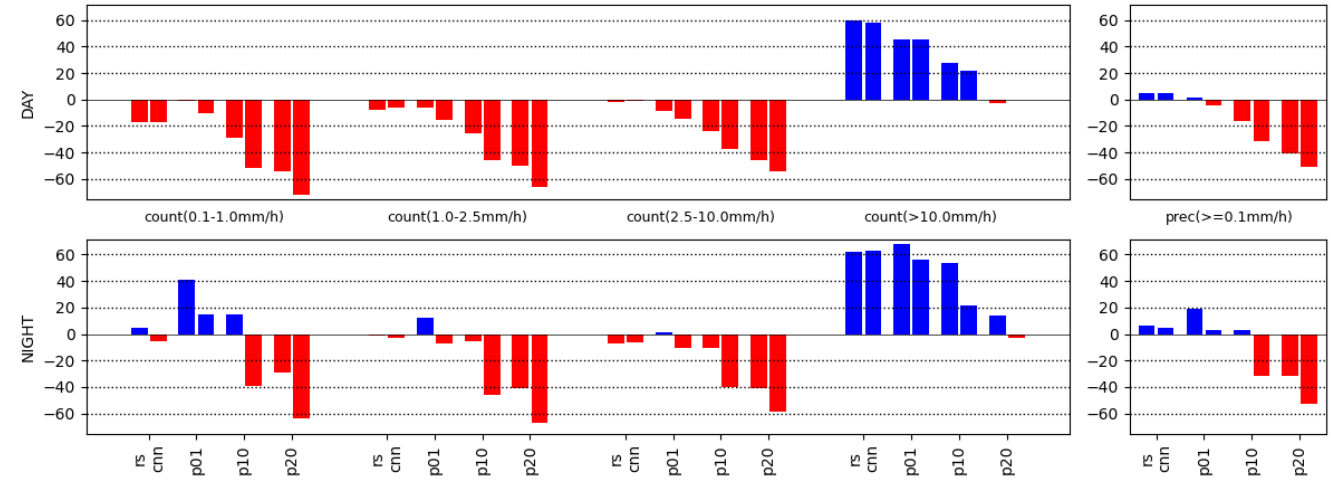

Figure 4. Percentage deviation of CML with the rain event detections *RS*, *CNN* as well as the SEVIRI probabilities represented by PC (left bars) and PC-Ph (right bars) *P01* till *P20* and *RADKLIM-YW* for counts per intensity class and precipitation amount for day (top) and night (bottom). Blue (resp. red) columns indicate overestimations (resp. underestimations) of CML data sets.

data sets as well as SEVIRI *P01* and *PC10* (left column of p10) agreed very well with *RADKLIM-YW*. *PC-Ph10* (right column of p10) and especially p20 tended to underestimate precipitation amounts. Based on these results, a performance similar to that of the TSB data sets was to be expected from the SEVIRI data.

4.2.2 Performance measures based on the confusion matrix

Based on the confusion matrix, the MCC was chosen as a meaningful criterion for performance with regard to rainfall intensity, differences between the two SEVIRI products as well as day and night differences. Again, there was a subdivision into intensity classes. The analysis was carried out for the TSB data sets *RS* and *CNN* and for the three lowest thresholds of PC and PC-Ph (.1, 10 and 20) (Fig.5). The lowest MCC was found for rain intensities below 2.5 mm/h (first two blocks), which illustrates the difficulty of rain event detection for CML data. This was particularly important as these low intensities made up a large amount of all rainfall and therefore dominated the mean statistical measures. Both TSB and ADB approaches naturally show weaknesses for light rain. TSB methods have to distinguish between precipitation signal and noise and the ADB method with SEVIRI data has to distinguish between precipitation and non-precipitating clouds. For higher intensities all rain event detection methods were robust. The best performance and highest MCC values were observed for moderate rain where precipitation signals are clearly visible in the CML time series and hardly any convective and small-scale precipitation is involved, which is more difficult to detect.

Comparing both SEVIRI products, PC performed slightly better than PC-Ph for most intensities and precipitation probabilities. The pre-analysis in Chapter 4.1 showed different results. The reason for this deviant behaviour is that for the latter case, the combination of CML signals and the SEVIRI product was responsible for the performance. *P01* for instance showed too

https://doi.org/10.5194/amt-2023-175
Preprint. Discussion started: 4 October 2023

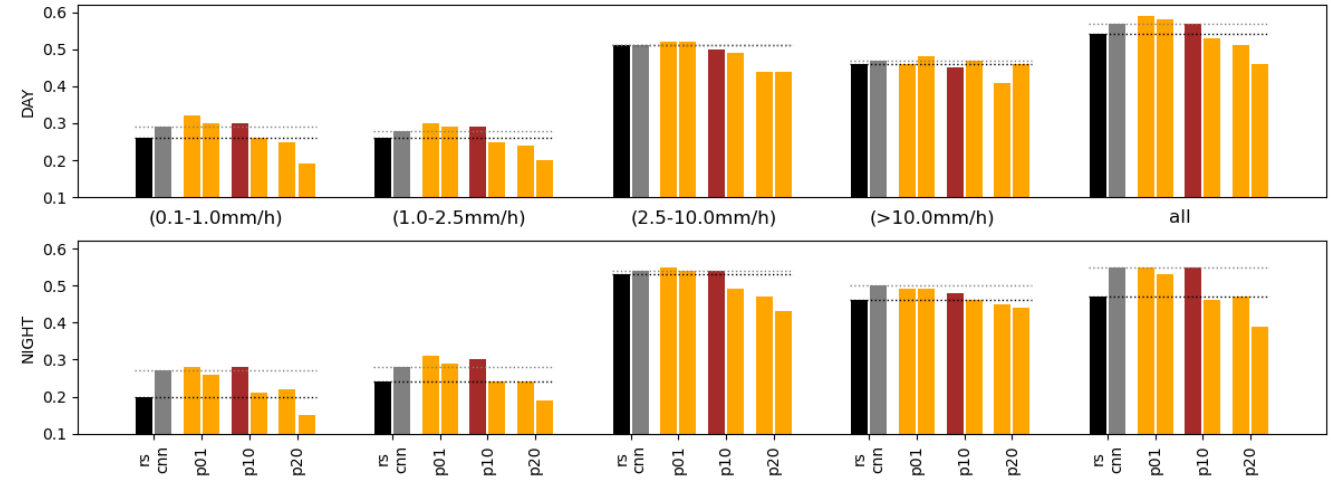

Figure 5. Same CML data sets and classes as in Fig. 4 but showing the MCC compared to *RADKLIM-YW*. *PC10* will be applied for further evaluations and is marked in brown.

many wet time steps but provided very good results when applied as a wet/dry indicator. The probability threshold had a larger influence on the rain event detection and hence the performance of the product than the differences between PC and PC-Ph.

In general, *CNN* performed better than *RS* for all intensities as shown by Polz et al. (2020) for a different period. SEVIRI performed better for smaller probability thresholds. Probabilities of 20 % and above (not shown here) usually showed even worse results than *RS*. In contrast, *P01* performed at least as well as *CNN*, usually even better.

At night, the results of *RS* were worse than during the day. This was most notable for small intensities. One reason could be dew formation on the CML radomes causing an increasing signal attenuation due to increasing number and size of droplets on the radomes. The *RS* method is only partially capable of distinguishing between such dewing events and precipitation. *CNN* did not show differences between day and night because it coped better with this issue. The SEVIRI-based products also showed slightly worse results for nighttime, but this was probably more due to the lack of three SEVIRI channels in the VIS and NIR at night. The calculation of microphysical variables is mainly based on those channels. Their absence consequently limits the reliability of all derived precipitation products. Differences between day and night already became apparent for the same precipitation probability with usually wetter nights. Additionally, ADB methods such as SEVIRI's wet/dry indicators are more independent from noise and artefacts in the CML time series. Hence, they were less affected by dew than TSB methods.

SEVIRI-based rain event detection with probabilities up to 10 % provided a at least similar performance as the *CNN* method and showed significant improvements compared to the *RS* method. *PC10* (marked in brown) showed the best performance when combining with the CNN method (described and shown in the next section) and is thus used as a new ADB method for all final results in the following sections.

https://doi.org/10.5194/amt-2023-175
Preprint. Discussion started: 4 October 2023


Atmospheric Measurement Techniques Discussions

4.3 Combinations

The main goal of this study is to improve the rain event detection compared to the conventional methods. This can be achieved by combining the advantages of different methods and overcoming certain disadvantages in this way. The main principle is to use a robust rain event detection, which performed well over all analysed metrics and rain intensity classes, as a first estimate. Next, very conservative (liberal) rain event detection methods were used to derive time steps with high confidence of being wet (dry) and replaced the time step from the previous estimate. For example, wet time steps were taken from a conservative method which had only few but trustworthy wet time steps. Based on our data, the following five processing steps (see Fig. 2) and the order thereof turned out to provide best results:

1. Either *CNN*, *PC01*, *PC10*, *PC-Ph01* or *PC-Ph10* served as a first estimate (typical individual method for rain event detection)
2. Additional dry time steps were derived from the very wet SEVIRI variant *PC01* or *PC-Ph01*.
3. Additional wet time steps were based on the very dry variant of *CNN* with a threshold of 0.94.
4. Further wet time steps were derived from SEVIRI with a precipitation probability of at least 30 % (PC30 or PCPh30).
5. Finally, time steps were assigned dry, which were dry based on *CNN* with a threshold of 0.1 (very wet variant).

The combinations are either based on PC or PC-Ph to minimize the expense of data processing. If a SEVIRI data set is chosen as the first estimate, Step 2 has no effect on the selection of wet and dry time steps.

Figure 6 shows how the TRSL (top) was interpreted by different rain event detection methods for an arbitrary CML and 5 days. The *CNN* led to an overestimation of wet time steps and to more precipitation than radar data showed. *PC10* was much dryer with a tendency of underestimation of wet time steps. *PC10all* was a combination applying *PC10* as a first estimate in step 1 of building a combination. It can also visually be regarded as a combination of the other two rain event detection methods.

To assess the quality and the potential of combinations, the following analysis were performed: First, the best of six combinations were chosen based on the MCC. Then the selected combination, a TSB data set and a ADB data set were compared in-depth, based on differences of TP, FP and FN with rain intensity. Finally, the performance of these three data sets was evaluated with regard to individual CMLs.

4.3.1 MCC of combinations

In order to evaluate the performance of combinations, the MCC of the TSB data sets and six different combinations are plotted in Fig. 7, again the variant with PC on the left and with PC-Ph on the right. *call* means combination applying *CNN* in the first step of building a combination and *p01all* and *p10all* the SEVIRI data with probabilities of 0.1 % and of 10 % respectively.

The improvements by combining rain event detection methods became obvious for light precipitation with an increase of the MCC between 0.3 and 0.1 for the lowest intensity classes. There was only minimal improvement for moderate precipitation, and no improvement for heavy precipitation. The main difference among the combinations is that PC data performs better than PC-Ph especially for lowest intensities and as a result of the large number of time steps there, also for the total class

https://doi.org/10.5194/amt-2023-175
Preprint. Discussion started: 4 October 2023

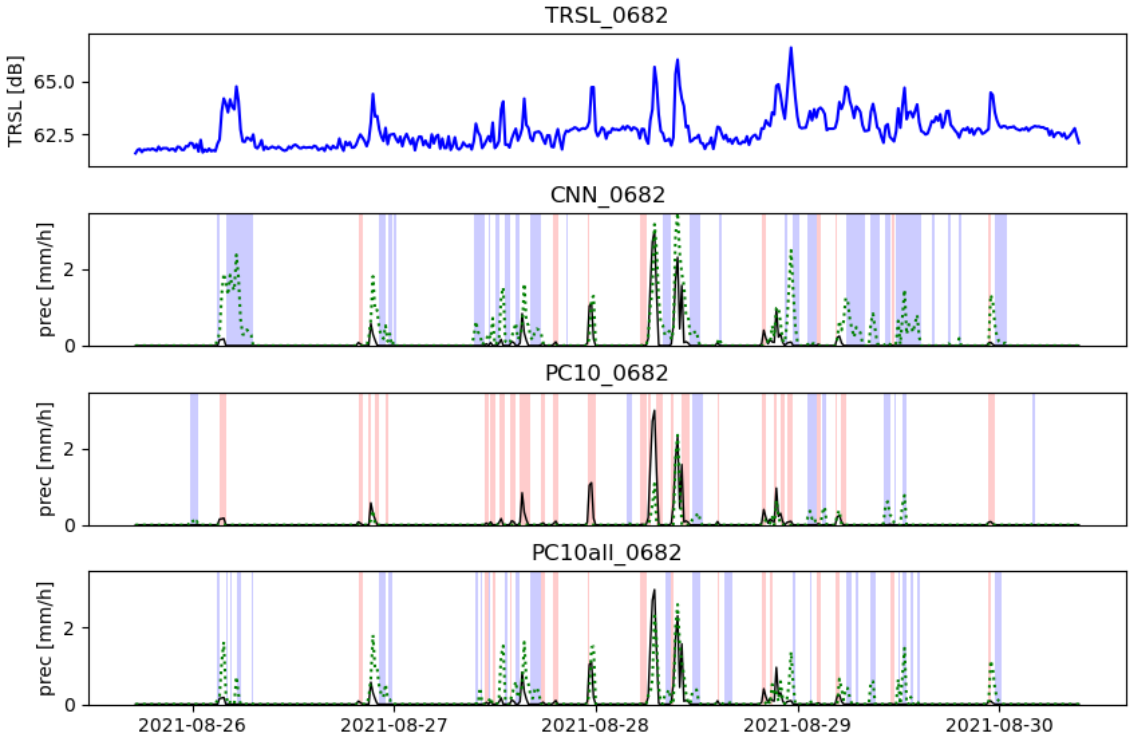

Figure 6. Example time series of a CML for 5 days. Raw TRSL (top) and *CNN*, *PC10* and *PC10all* (green line) are opposed to *RADKLIM-YW* (black line). Wet time steps which are assigned dry by CML (FN) are marked shaded red and dry time steps which are assigned wet (FP) are marked shaded blue.

335 (*all*). Very similar results were obtained for the night. Again, PC performed slightly better than PC-Ph and combinations were superior to the applied TSB data sets. The combination *PC10all* (marked in brown) showed the largest overall improvements with a MCC of 0.62 compared to 0.57 (*CNN*) and 0.54 (*RS*) at daytime and 0.6 compared to 0.55 (*CNN*) and 0.47 (*RS*) at nighttime. Combinations are most effective for the very low intensities where the largest uncertainties of individual methods were observed. For individual methods, there is often a trade-off between few FN (liberal) or few FP (conservative) that might
340 not be necessary when applying two data sets. Analyzing the same time steps or time series by different methods likely increases the reliability of a resulting rain event detection. In the following, we concentrate on *PC10all* to evaluate the performance of such a combination in more depth.

https://doi.org/10.5194/amt-2023-175
Preprint. Discussion started: 4 October 2023

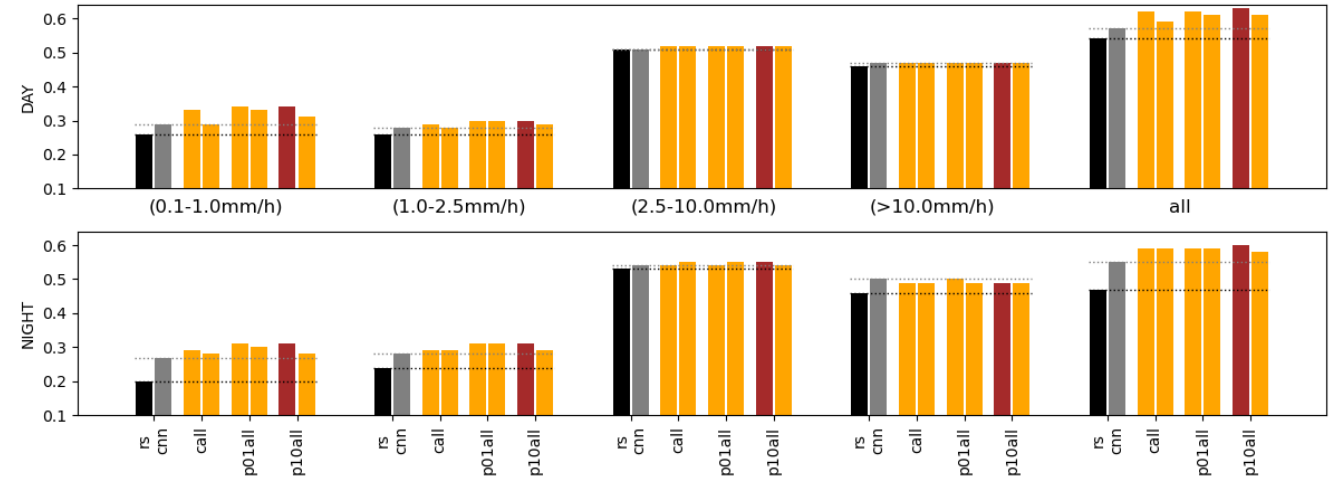

Figure 7. Same as Fig. 4 but for the combinations where *CNN* (*call*) and PC/PC-Ph with thresholds *P01* (*p01all*) and *P10* (*p10all*) serve as the first estimate. *PC10all* will be applied for further evaluations and is marked in brown.

4.3.2 Performance of confusion matrix values vs. intensity

In order to be able to understand what distinguishes the individual methods for rain event detection, the distribution of TP, FP and FN is plotted against intensity and shown for frequency of occurrence (top) and total precipitation (bottom) in Fig. 8. The left column show those distributions for the *CNN* method. The other columns reveal the corresponding differences between *PC10* and *CNN* (middle) and between the combination *PC10all* and *CNN* (right) for day and night. In summary, a typical TSB method (*CNN*), a new ADB method (*PC10*) and a combination thereof (*PC10all*) were compared.

According to Fig.8a (middle), *PC10* is drier than *CNN* with less TP. Improvements were achieved by a decrease in FP but also a similarly large increase in FN during the day showed up. The results for the combination were different. Here, the desired effect of a general improvement became apparent: both FP and FN decreased for all intensities. TP and thus precipitation were slightly increased.

At night, *PC10* is much wetter than during the day with an increase of TP and a decrease of FN compared to *CNN*. For intensities below 0.5 mm/h, there was a massive increase of FP, but not for higher intensities. The combination *PC10all* also shows this SEVIRI issue, however, to a lesser extent. There are clear improvements for all intensities, except for intensities below 0.5 mm/h where FP was also increased compared to *CNN*. Since nights were usually wetter based on SEVIRI data, a larger precipitation probability than 10 % to reduce FPs from SEVIRI might lead to overall improvements, but this was not tested in this investigation.

https://doi.org/10.5194/amt-2023-175
Preprint. Discussion started: 4 October 2023

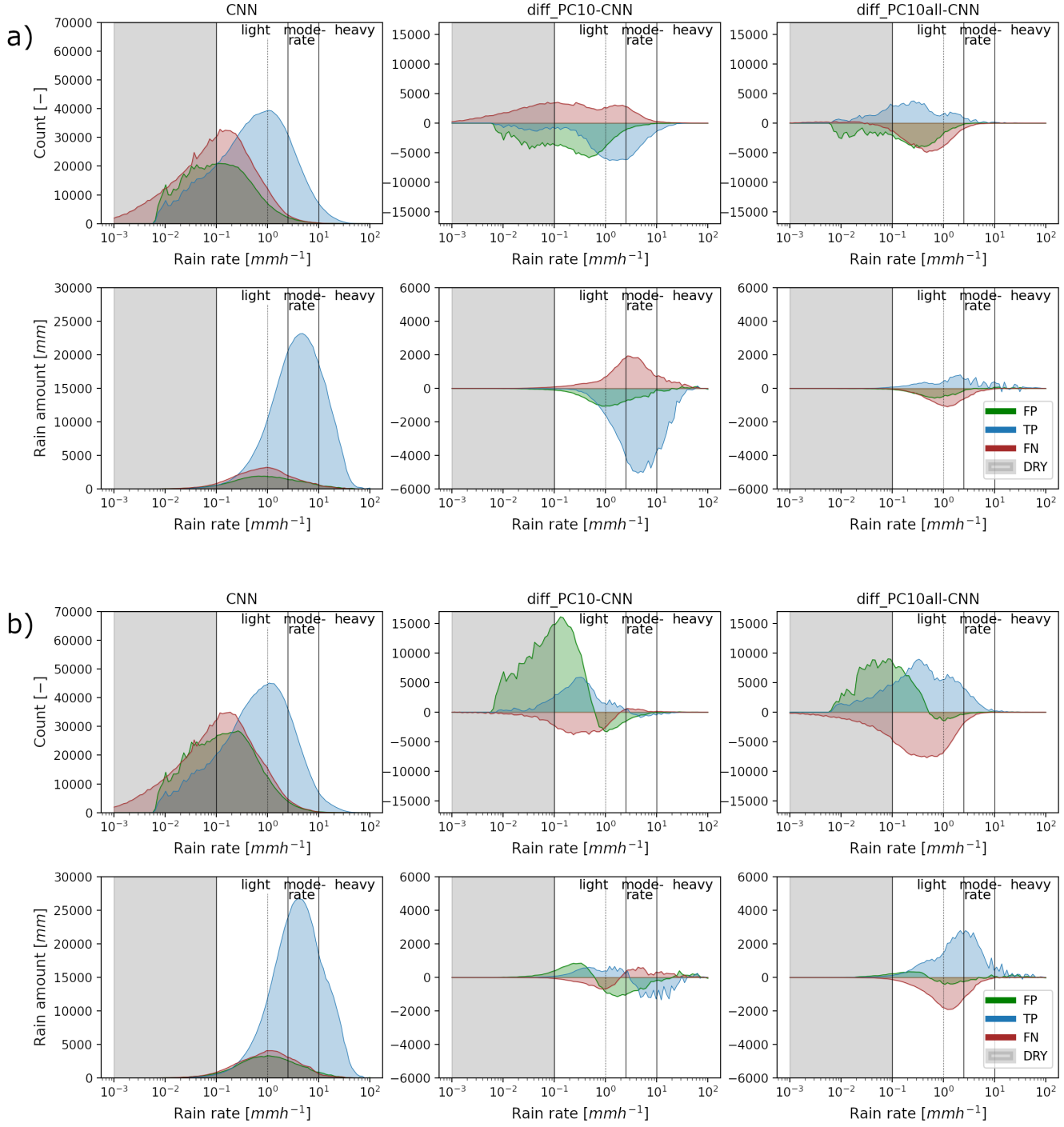

Figure 8. Top: The number of FP, TP, and FN time steps with a specific rain rate are compared for *CNN* (left) and the respective amount of rainfall (bottom). *diff_PC10-CNN* reveal the respective differences between *PC10* and *CNN* (middle) and *diff_PC10all-CNN* between *PC10all* and *CNN* (right). a) is daytime and b) is nighttime. The rain intensities for FP and TP are estimated by the CML, while the rain intensities for FN are taken from the reference.

https://doi.org/10.5194/amt-2023-175
Preprint. Discussion started: 4 October 2023


Atmospheric Measurement Techniques Discussions

4.4 Influence of chosen rain event detection method on individual CMLs

The results so far were based on averaged metrics over all CMLs. The performance of individual CMLs might, however, differ from this mean behaviour and systematic differences between well and worse performing CMLs are possible for different rain event detection methods. Therefore, scatterplots of different rain event detection methods and combinations against the *CNN* method for ACC, MCC and PCC show the change of performance of each CML in Fig.9. *PC10* and *PC10all* are compared with *CNN* for day and night.

The differences between *PC10* and *CNN* were small. No systematic differences were found using PCC. Based on ACC, the majority of CMLs are slightly improved by *PC10* including the worst performing ones. Regarding MCC, the overall performance is equal for *CNN* and *PC10*, only the worst performing ones were almost always improved here, too. A very similar picture emerged at night, with improvements in particular for the worst performing ones. These CMLs with low performance usually showed a high level of noise which is similar to the signal fluctuations caused by rainfall. Consequently, the separation of precipitation signals is difficult for all TSB methods. The fact that ADB methods are independent from the CML time series is responsible for this improvement based on SEVIRI data. The combination *PC10all* showed clear improvements for ACC and MCC compared to *CNN* for daytime and nighttime. Almost all CMLs were improved by the combination compared to individual methods for rain event detection and especially the worse performing ones.

5 Conclusions

In this study we aimed to address the questions whether satellite-derived precipitation products are suitable indicators for the rain event detection in CML data with respect to day/night differences and rain intensities and whether combinations of TSB and ADB methods show an additional added value. We achieved this by using PC and PC-Ph from MSG SEVIRI in an ADB rain event detection and compared the results to two TSB rain event detection methods. Then we combined the most promising variants in such a way that the most confident detection method was used for any given time step.

The results clearly show that PC and PC-Ph products from MSG SEVIRI can be used for the detection of rain events in CML attenuation time series. They performed even better than RS, one of the most commonly used rain event detection methods and similar to the sophisticated CNN method. Minor differences between the SEVIRI products PC and PC-Ph exist, but the applied precipitation probability dominated the overall behaviour. An improved PC-Ph product has been available since April 2022 potentially making its application in rain event detection even more attractive (personal communication with NWC SAF).

However, the performance of ADB methods based on SEVIRI were worse at night than during the day due to the lack of the three SEVIRI channels (VIS and NIR). Since CNN did not show a decrease of quality at night, it would be logical to vary the rain event detection for day and night time. We did not aim for such a temporal variation because the differences between CNN and ADB methods at night were negligible, to keep computational effort low and to avoid inconsistencies in the resulting time series. Compared to the ADB and CNN, the RS method can only partly be recommended. Especially at nighttime, when dew formation on radomes is probably responsible for false positive rain event detection and therefore a decrease of quality.

https://doi.org/10.5194/amt-2023-175
Preprint. Discussion started: 4 October 2023

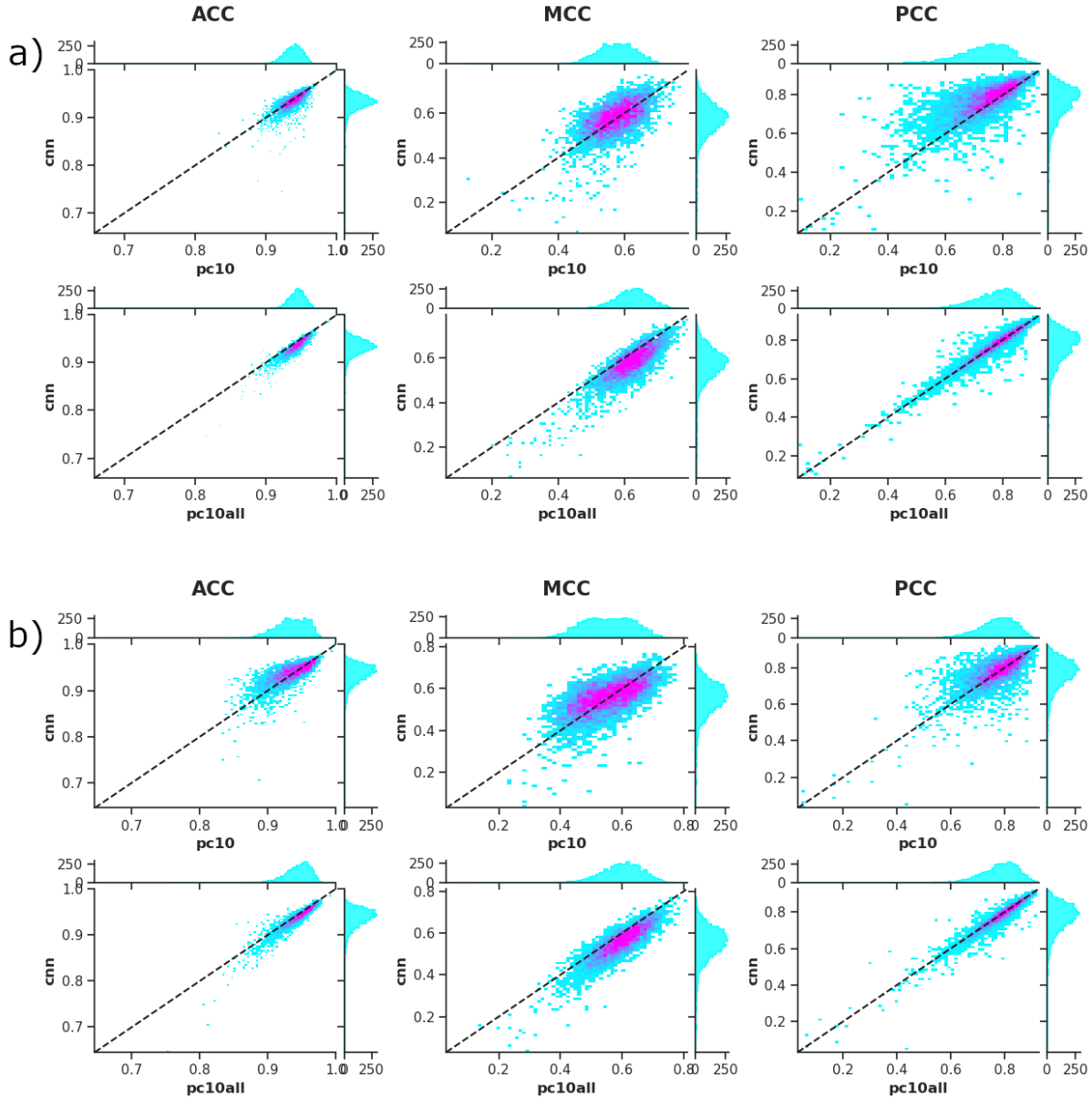

Figure 9. Scatter density of *PC10* (top) and *PC10all* (bottom) versus *CNN* for ACC (left), MCC (middle) and PCC (right) for a) day and b) night.

https://doi.org/10.5194/amt-2023-175
Preprint. Discussion started: 4 October 2023


Atmospheric Measurement Techniques Discussions

The quality of the rain event detection clearly depended on the rain intensity, with a better performance for moderate and heavy rain than for light rain. For flood forecasting light rain is often negligible but this is not the case for water balance analyses. Additionally, the increasing threat of droughts in context to climate change also requires a high-quality representation of light rain. Low precipitation intensities show the largest potential for improvement and the main differences in this study were also obtained there.

The effort to use ADB is larger than for TSB methods because the processing of additional needed satellite data sets can be time consuming. With stepwise combinations, as presented here, the effort increases accordingly. The shown additional improvements by combinations are promising and justify the effort. We expect added value of combinations also for other regions or different kinds of CML data sets. However, thresholds and the order of correction steps might vary, there. The multitude of possibilities when combining different rain event detection methods is particularly interesting. Varying methods or thresholds depending on data quality or rainfall intensity is also possible.

In principle, combinations from two TSB methods are possible and may lead to improvements. However, we recommend applying a combination of TSB and ADB methods to exploit the advantages of both approaches: TSB methods are easy to apply and provide precise results where the separation of noise and precipitation signals is obvious. Whereas, ADB methods show a better performance for noisy or unstable CML time series due to their independence from the actual CML signal. Burkina Faso for example has only few rainfall stations, but several hundred CMLs. Most CMLs outside the capital Ouagadougou are long (>20km) and use frequencies around 7 GHz. Their time series are quite noisy and show large fluctuations from other sources than rain. With abundant information from geostationary satellites and the methods presented in this work, we expect to extract useful ground-based rainfall information from such CMLs in this region with scarce rainfall data.

Data availability. CML data were provided by Ericsson Germany and are not publicly available. RADKLIM-YW was provided by the German Weather Service (DWD) and are publicly available.: https://opendata.dwd.de/climate_environment/CDC/grids_germany/5_minutes/radolan (last access: 28 July 2023; DWD CDC, 2023)

Author contributions. AW and CC designed the study layout, and AW carried it out with contributions of CC, MG and JP. Data and related support was provided by LL and JAL. AW prepared the article with contributions from all co-authors.

Competing interests. The authors declare that they have no conflict of interest.

Acknowledgements. We thank Ericsson for their support and cooperation in the acquisition of the CML data. This research has been supported by the Federal Ministry of Education and Research (Grants 01LZ1904A-C and 13N16432), the Helmholtz Association (Grant ZT-0025) and the German Research Foundation (Grant CH-1785/1-2).

https://doi.org/10.5194/amt-2023-175
Preprint. Discussion started: 4 October 2023

Atmospheric Measurement Techniques Discussions

References

Atlas, D.: Radar in Meteorology - Battan Memorial and 40th Anniversary Radar Meteorology Conference, Amer. Meteor. Soc., 1990.

Atlas, D. and Ulbrich, C. W.: Path- and Area-Integrated Rainfall Measurement by Microwave Attenuation in the 1–3 cm Band, Journal of Applied Meteorology and Climatology, 16, 1322 – 1331, https://doi.org/10.1175/1520-0450(1977)016<1322:PAAIRM>2.0.CO;2, 1977.

Bartels, H., Weigl, E., Reich, T., Lang, P., Wagner, A., Kohler, O., and Gerlach, N.: Projekt RADOLAN - Routineverfahren zur Online-Aneichung der Radarniederschlagsdaten mit Hilfe von automatischen Bodenniederschlagsstationen (Ombrometer), Deutscher Wetterdienst, Hydrometeorologie, 2004.

Bruni, G., Reinoso, R., van de Giesen, N. C., Clemens, F. H. L. R., and ten Veldhuis, J. A. E.: On the sensitivity of urban hydrodynamic modelling to rainfall spatial and temporal resolution, Hydrology and Earth System Sciences, 19, 691–709, https://doi.org/10.5194/hess-19-691-2015, 2015.

Chwala, C. and Kunstmann, H.: Commercial microwave link networks for rainfall observation: Assessment of the current status and future challenges, WIREs Water, 6, e1337, https://doi.org/https://doi.org/10.1002/wat2.1337, e1337 WATER-363.R2, 2019.

Chwala, C., Gmeiner, A., Qiu, W., Hipp, S., Nienaber, D., Siart, U., Eibert, T., Pohl, M., Seltmann, J., Fritz, J., and Kunstmann, H.: Precipitation observation using microwave backhaul links in the alpine and pre-alpine region of southern Germany, Hydrol. Earth Syst. Sci., 16, 2647–2661, 2012.

Chwala, C., Keis, F., and Kunstmann, H.: Real-time data acquisition of commercial microwave link networks for hydrometeorological applications, Atmospheric Measurement Techniques, 9, 991–999, https://doi.org/10.5194/amt-9-991-2016, 2016.

Cristiano, E., ten Veldhuis, M.-C., and van de Giesen, N.: Spatial and temporal variability of rainfall and their effects on hydrological response in urban areas – a review, Hydrology and Earth System Sciences, 21, 3859–3878, https://doi.org/10.5194/hess-21-3859-2017, 2017.

DWD: German Met. Service Glossary, German Meteorological Service, 'https://www.dwd.de/DE/service/lexikon/Functions/glossar.html?lv2=101812&lv3=101906', (last access: 28 July 2023), 2023.

D'Amico, M., Manzoni, A., and Solazzi, G. L.: Use of Operational Microwave Link Measurements for the Tomographic Reconstruction of 2-D Maps of Accumulated Rainfall, IEEE Geoscience and Remote Sensing Letters, 13, 1827–1831, https://doi.org/10.1109/LGRS.2016.2614326, 2016.

Fu, S., Sonnenborg, T. O., Jensen, K. H., and He, X.: Impact of Precipitation Spatial Resolution on the Hydrological Response of an Integrated Distributed Water Resources Model, Vadose Zone J., 10, 25–36, 2011.

Graf, M., Chwala, C., Polz, J., and Kunstmann, H.: Rainfall estimation from a German-wide commercial microwave link network: optimized processing and validation for 1 year of data, Hydrology and Earth System Sciences, 24, 2931–2950, https://doi.org/10.5194/hess-24-2931-2020, 2020.

Graf, M., El Hachem, A., Eisele, M., Seidel, J., Chwala, C., Kunstmann, H., and Bárdossy, A.: Rainfall estimates from opportunistic sensors in Germany across spatio-temporal scales, Journal of Hydrology: Regional Studies, 37, 100 883, https://doi.org/https://doi.org/10.1016/j.ejrh.2021.100883, 2021.

Habi, H. V. and Messer, H.: Wet-Dry Classification Using LSTM and Commercial Microwave Links, in: 2018 IEEE 10th Sensor Array and Multichannel Signal Processing Workshop (SAM), pp. 149–153, https://doi.org/10.1109/SAM.2018.8448679, 2018.

https://doi.org/10.5194/amt-2023-175
Preprint. Discussion started: 4 October 2023

Haese, B., Hörning, S., Chwala, C., Bárdossy, A., Schalge, B., and Kunstmann, H.: Stochastic Reconstruction and Interpolation of Precipitation Fields Using Combined Information of Commercial Microwave Links and Rain Gauges, Water Resources Research, 53, 10 740–10 756, https://doi.org/https://doi.org/10.1002/2017WR021015, 2017.

Hernanz, A., Lahuerta García, J. A., Calbet, X., and Rípodas, P.: Algorithm Theoretical Basis Document for the Precipitation Product Processors of the NWC/GEO, NWCSAF, https://www.nwcsaf.org/Downloads/GEO/2021/Documents/Scientific_Docs/NWC-CDOP3-GEO-AEMET-SCI-ATBD-Precipitation_v1.0.1.pdf, (last access: 28 July 2023), 2019.

Hou, A. Y., Kakar, R. K., Neeck, S., Azarbarzin, A. A., Kummerow, C. D., Kojima, M., Oki, R., Nakamura, K., and Iguchi, T.: The Global Precipitation Measurement Mission, Bull. Amer. Meteorol. Soc., 95, 701–722, 2014.

ITU-R: Specific attenuation model for rain for use in prediction methods (Recommendation P.838-3), ITU-R, https://www.itu.int/rec/R-REC-P.838-3-200503-I/en, (last access: 28 July 2023), 2005.

Kreklow, J., Tetzlaff, B., Burkhard, B., and Kuhnt, G.: Radar-Based Precipitation Climatology in Germany—Developments, Uncertainties and Potentials, Atmosphere, 11, https://doi.org/10.3390/atmos11020217, 2020.

Kumah, K., Maathuis, B., Hoedjes, J., and Su, Z.: Near real-time estimation of high spatiotemporal resolution rainfall from cloud top properties of the MSG satellite and commercial microwave link rainfall intensities, Atmospheric Research, 279, 106 357, https://doi.org/https://doi.org/10.1016/j.atmosres.2022.106357, 2022.

Kumah, K. K., Hoedjes, J. C. B., David, N., Maathuis, B. H. P., Gao, H. O., and Su, B. Z.: The MSG Technique: Improving Commercial Microwave Link Rainfall Intensity by Using Rain Area Detection from Meteosat Second Generation, Remote Sensing, 13, https://doi.org/10.3390/rs13163274, 2021.

Lahuerta García, J. A.: Scientific and Validation Report for the Precipitation Product Processors of the NWC/GEO, Agencia Estatal de Meteorología, https://www.nwcsaf.org/AemetWebContents/ScientificDocumentation/Documentation/GEO/v2016/NWC-CDOP2-GEO-AEMET-SCI-VR-Precipitation_v1.0.pdf, (last access: 28 July 2023), 2019.

Lahuerta García, J. A.: Algorithm theoretical basis document for the precipitation product processors of the NWC/-GEO, Agencia Estatal de Meteorología, https://www.nwcsaf.org/Downloads/GEO/2021/Documents/Scientific_Docs/NWC-CDOP3-GEO-AEMET-SCI-ATBD-Precipitation_v1.0.1.pdf, (last access: 28 July 2023), 2021.

Leijnse, H., Uijlenhoet, R., and Stricker, J. N. M.: Rainfall measurement using radio links from cellular communication networks, Water Resources Research, 43, https://doi.org/https://doi.org/10.1029/2006WR005631, 2007.

Leijnse, H., Uijlenhoet, R., and Stricker, J.: Microwave link rainfall estimation: Effects of link length and frequency, temporal sampling, power resolution, and wet antenna attenuation, Advances in Water Resources, 31, 1481–1493, https://doi.org/https://doi.org/10.1016/j.advwatres.2008.03.004, hydrologic Remote Sensing, 2008.

Liberman, Y., Samuels, R., Alpert, P., and Messer, H.: New algorithm for integration between wireless microwave sensor network and radar for improved rainfall measurement and mapping, Atmospheric Measurement Techniques, 7, 3549–3563, https://doi.org/10.5194/amt-7-3549-2014, 2014.

Maggioni, V., Meyers, P. C., and Robinson, M. D.: A Review of Merged High-Resolution Satellite Precipitation Product Accuracy during the Tropical Rainfall Measuring Mission (TRMM) Era, Journal of Hydrometeorology, 17, 1101 – 1117, https://doi.org/10.1175/JHM-D-15-0190.1, 2016.

Messer, H. and Sendik, O.: A New Approach to Precipitation Monitoring: A critical survey of existing technologies and challenges, IEEE Signal Processing Magazine, 32, 110–122, https://doi.org/10.1109/MSP.2014.2309705, 2015.

https://doi.org/10.5194/amt-2023-175
Preprint. Discussion started: 4 October 2023

Atmospheric Measurement Techniques Discussions

Messer, H., Zinevich, A., and Alpert, P.: Environmental Monitoring by Wireless Communication Networks, Science, 312, 713–713, https://doi.org/10.1126/science.1120034, 2006.

Overeem, A., Leijnse, H., and Uijlenhoet, R.: Measuring urban rainfall using microwave links from commercial cellular communication networks, Water Resources Research, 47, https://doi.org/https://doi.org/10.1029/2010WR010350, 2011.

Overeem, A., Leijnse, H., and Uijlenhoet, R.: Country-wide rainfall maps from cellular communication networks, Proceedings of the National Academy of Sciences, 110, 2741–2745, https://doi.org/10.1073/pnas.1217961110, 2013.

Overeem, A., Leijnse, H., and Uijlenhoet, R.: Two and a half years of country-wide rainfall maps using radio links from commercial cellular telecommunication networks, Water Resources Research, 52, 8039–8065, https://doi.org/https://doi.org/10.1002/2016WR019412, 2016.

Pollock, M. D., O'Donnell, G., Quinn, P., Dutton, M., Black, A., Wilkinson, M. E., Colli, M., Stagnaro, M., Lanza, L. G., Lewis, E., Kilsby, C. G., and O'Connell, P. E.: Quantifying and Mitigating Wind-Induced Undercatch in Rainfall Measurements, Water Resources Research, 54, 3863–3875, https://doi.org/https://doi.org/10.1029/2017WR022421, 2018.

Polz, J., Chwala, C., Graf, M., and Kunstmann, H.: Rain event detection in commercial microwave link attenuation data using convolutional neural networks, Atmospheric Measurement Techniques, 13, 3835–3853, https://doi.org/10.5194/amt-13-3835-2020, 2020.

Rafieeinasab, A., Norouzi, A., Kim, S., Habibi, H., Nazari, B., Seo, D.-J., Lee, H., Cosgrove, B., and Cui, Z.: Toward high-resolution flash flood prediction in large urban areas – Analysis of sensitivity to spatiotemporal resolution of rainfall input and hydrologic modeling, Journal of Hydrology, 531, 370–388, https://doi.org/https://doi.org/10.1016/j.jhydrol.2015.08.045, hydrologic Applications of Weather Radar, 2015.

Rios Gaona, M. F., Overeem, A., Leijnse, H., and Uijlenhoet, R.: Measurement and interpolation uncertainties in rainfall maps from cellular communication networks, Hydrology and Earth System Sciences, 19, 3571–3584, https://doi.org/10.5194/hess-19-3571-2015, 2015.

Roebeling, R. A. and Holleman, I.: SEVIRI rainfall retrieval and validation using weather radar observations, Journal of Geophysical Research: Atmospheres, 114, https://doi.org/https://doi.org/10.1029/2009JD012102, 2009.

Roebeling, R. A., Deneke, H. M., and Feijt, A. J.: Validation of Cloud Liquid Water Path Retrievals from SEVIRI Using One Year of CloudNET Observations, Journal of Applied Meteorology and Climatology, 47, 206 – 222, https://doi.org/https://doi.org/10.1175/2007JAMC1661.1, 2008.

Roversi, G., Alberoni, P. P., Fornasiero, A., and Porcù, F.: Commercial microwave links as a tool for operational rainfall monitoring in Northern Italy, Atmospheric Measurement Techniques, 13, 5779–5797, https://doi.org/10.5194/amt-13-5779-2020, 2020.

Schleiss, M. and Berne, A.: Identification of Dry and Rainy Periods Using Telecommunication Microwave Links, IEEE Geoscience and Remote Sensing Letters, 7, 611–615, https://doi.org/10.1109/LGRS.2010.2043052, 2010.

Schleiss, M., Olsson, J., Berg, P., Niemi, T., Kokkonen, T., Thorndahl, S., Nielsen, R., Ellerbæk Nielsen, J., Bozhinova, D., and Pulkkinen, S.: The accuracy of weather radar in heavy rain: a comparative study for Denmark, the Netherlands, Finland and Sweden, Hydrology and Earth System Sciences, 24, 3157–3188, https://doi.org/10.5194/hess-24-3157-2020, 2020.

Schmid, J.: The SEVIRI instrument, in: Proceedings of the 2000 EUMETSAT meteorological satellite data user's conference, Bologna, Italy, vol. 29, pp. 13–32, 2000.

Sevruk, B.: Rainfall Measurement: Gauges, chap. 35, John Wiley & Sons, Ltd, https://doi.org/https://doi.org/10.1002/0470848944.hsa038, 2006.

Song, K., Liu, X., Zou, M., Zhou, D., Wu, H., and Ji, F.: Experimental Study of Detecting Rainfall Using Microwave Links: Classification of Wet and Dry Periods, IEEE Journal of Selected Topics in Applied Earth Observations and Remote Sensing, 13, 5264–5271, https://doi.org/10.1109/JSTARS.2020.3021555, 2020.

https://doi.org/10.5194/amt-2023-175
Preprint. Discussion started: 4 October 2023

Steiner, M., Smith, J. A., and Uijlenhoet, R.: A Microphysical Interpretation of Radar Reflectivity-Rain Rate Relationships, J. Atmos. Sci., 61, 1114–1131, 2004.

Thoss, A.: Algorithm Theoretical Basis Document for Precipitating Clouds of the NWC/PPS, NWCSAF, https://www.nwcsaf.org/AemetWebContents/ScientificDocumentation/Documentation/PPS/v2014/NWC-CDOP2-PPS-SMHI-SCI-ATBD-4_v1_0.pdf, (last access: 28 July 2023), 2014.

Uijlenhoet, R., Steiner, M., and Smith, J. A.: Variability of Raindrop Size Distributions in a Squall Line and Implications for Radar Rainfall Estimation, J. Hydrometeor., 4, 43–61, 2003.

Uijlenhoet, R., Overeem, A., and Leijnse, H.: Opportunistic remote sensing of rainfall using microwave links from cellular communication networks, WIREs Water, 5, e1289, https://doi.org/https://doi.org/10.1002/wat2.1289, 2018.

van de Beek, R. C. Z. ., Olsson, J., and Andersson, J.: Optimal grid resolution for precipitation maps from commercial microwave link networks, Advances in Science and Research, 17, 79–85, https://doi.org/10.5194/asr-17-79-2020, 2020.

van het Schip, T. I., Overeem, A., Leijnse, H., Uijlenhoet, R., Meirink, J. F., and van Delden, A. J.: Rainfall measurement using cell phone links: classification of wet and dry periods using geostationary satellites, Hydrological Sciences Journal, 62, 1343–1353, https://doi.org/10.1080/02626667.2017.1329588, 2017.

Villarini, G. and Krajewski, W. F.: Review of the Different Sources of Uncertainty in Single Polarization Radar-Based Estimates of Rainfall, Surveys in Geophysics, 31, 107–129, https://doi.org/10.1007/s10712-009-9079-x, 2010.

Wagner, A.: Spatiotemporal Variability of Precipitation : Measurements - Simulations - Limitations, doctoralthesis, Universität Augsburg, https://opus.bibliothek.uni-augsburg.de/opus4/files/38014/Wagner_Diss.pdf, (last access: 28 July 2023), 2018.

Wagner, A., Seltmann, J., and Kunstmann, H.: Joint statistical correction of clutters, spokes and beam height for a radar derived precipitation climatology in southern Germany, Hydrol. Earth Syst. Sci., 16, 4101–4117, 2012.

Wang, Z., Schleiss, M., Jaffrain, J., Berne, A., and Rieckermann, J.: Using Markov switching models to infer dry and rainy periods from telecommunication microwave link signals, Atmospheric Measurement Techniques, 5, 1847–1859, https://doi.org/10.5194/amt-5-1847-2012, 2012.

Winterrath, T., Rosenow, W., and Weigl, E.: On the DWD quantitative precipitation analysis and nowcasting system for real-time application in German flood risk management, IAHS-AISH publication, pp. 323–329, 2012.

Winterrath, T., Brendel, C., Hafer, M., Junghänel, T., Klameth, A., Lengfeld, K., Walawender, E., Weigl, E., and Becker, A.: RADKLIM Version 2017.002: Reprocessed quasi gauge-adjusted radar data, 5-minute precipitation sums (YW), https://doi.org/10.5676/DWD/RADKLIM_YW_V2017.002, 2018.